Native-MS Analysis of Monoclonal Antibody Conjugates by Fourier Transform Ion Cyclotron Resonance Mass Spectrometry

Iain D. G Campuzano[1]*, Chawita Netirojjanakul[2], Michael Nshanian[3], Jennifer L. Lippens[1¶], David Kilgour[4], Steve Van Orden[5] and Joseph A. Loo[3]*

1. Discovery Attribute Sciences, Amgen, Thousand Oaks, CA, 91320, United States
2. Hybrid Modality Engineering, Amgen, Thousand Oaks, CA, 91320, United States
3. Department of Chemistry and Biochemistry, and Department of Biological Chemistry, University of California−Los Angeles, Los Angeles, California 90095, United States
4. Department of Chemistry and Forensics, Nottingham Trent University, Nottingham, NG11 8NS, United Kingdom
5. Bruker Daltonics Inc. Billerica, Massachusetts, 01821, United States

*Corresponding authors: Iain D. G, Campuzano, iainc@amgen.com and Joseph A. Loo, JLoo@chem.ucla.edu

¶Jennifer L. Lippens is an Amgen Post-Doctoral Research Fellow

Abstract

Antibody drug conjugates (ADCs) are an important class of therapeutic molecule currently being used to treat HER2-positive metastatic breast cancer, relapsed or refractory Hodgkin lymphoma, systemic anaplastic large cell lymphoma, relapsed or refractory B-cell precursor acute lymphoblastic leukemia and acute myeloid leukemia. An ADC typically consists of a small molecule or peptide-based cytotoxic moiety covalently linked, via lysine or cysteine residues, to amonoclonal antibody (mAb) scaffold. Mass spectrometric (MS) characterization of thesemolecules afford highly accurate molecular weight (MW) and drug-to-antibody ratio (DAR) determination, and is typically performed using orthogonal acceleration time-of-flight (oa-ToF) analysers and more recently Orbitrap instruments. Herein we describe for the first time the use of a 15 Tesla solariX Fourier transform ion cyclotron mass spectrometer to characterize an IgG1 mAb molecule conjugated with biotin via native lysine and cysteine residues, under native-MS and solution conditions. The cysteine biotin conjugates remained fully intact, demonstrating the ability of the FT-ICR to maintain the noncovalent interactions and efficiently transmit labile protein complexes. Native-MS was acquired and is displayed in magnitude mode using a symmetric Hann apodisation function. Baseline separation is achieved on all covalent biotin additions, for each charge state, for both the lysine and cysteine biotin-conjugates. Average DAR values obtained by native-MS for the lysine conjugate are compared to those derived by denaturing reversed phase liquid chromatography using an oa-ToF MS system (1.56 ±0.02 versus 2.24 ±0.02 for a 5-molar equivalent and 3.99 ±0.09 versus 4.43 ±0.01 for a 10-molar equivalent, respectively). Increased DAR value accuracy can be obtained for the higher biotin load, when using standard ESI conditions as opposed to nanoESI native-MS conditions.

Introduction

In recent years, antibody-drug conjugates (ADCs) have emerged as a promising class of protein therapeutics based on chemical conjugation technologies [1]. ADCs are designed for highly targeted delivery of a potent cytotoxic molecule to the tumour cell with minimal systemic toxicity [2]. Currently four ADCs, ado-Trastuzumab emtansine (Kadcyla; Genentech/Immunogen), Brentuximab vedotin (Adcetris; Seattle Genetics), Inotuzumab ozogamicin (Besponsa; Pfizer) and Gemtuzumab ozogamicin (Gemtuzumaba; Pfizer) have been approved by the US FDA. Moreover, there are more than 20 ADCs in various stages of clinical trials [3,4]. The current technology utilises lysine and cysteine modification of antibodies, in which the drug is conjugated to the antibody using a linker [5-8]. Lysine conjugation typically results in a distribution of drug-to-antibody ratio (DAR) ranging from 0 to 8 [5,9]. Cysteine conjugation can take place through covalent modification of an engineered cysteine residue [10] or a reduced inter-chain disulphide bond(s) [11] resulting in a DAR distribution incrementally increasing by two units (DAR= 0, 2, 4, 6 and 8) [11,12].

Analysis of proteins and macromolecular complexes under native-MS and solution conditions has predominantly focused on gas-phase structural biology [13-15] where native stoichiometry can be readily determined. However more recently, the combination of ion mobility and MS can provide additional shape information, in the form of an ion-neutral collision cross section value [16], where large levels of gas-phase collapse have been characterized for mAbs [17,18]. Advances in instrument design have further showcased MS analysis of mAbs [19,20], both native and denatured, using the Orbitrap analyser. Native-MS analysis of ADCs has been increasing over the past decade for a number of reasons, chief of which are that MS can provide highly accurate DAR values specifically determined under native-MS and solution conditions, critical for cysteine conjugates [11,21,22]. The FT-based Orbitrap instrument, typically the extended mass range Orbitrap [19,23] have been readily adopted in both industry and academia for the analysis of mAbs [19,24] and ADCs [24,25] under native-MS and solution conditions due to the Orbitraps exemplary data quality over that typically achieved on oa-ToF instruments [18,19,25] and now high mass transmission capabilities [19,23,24,26]. Over the past 5 years a number of groups have used Fourier transform ion cyclotron resonance (FT-ICR) instrumentation to analyse mAbs under native [27]

and denaturing [28,29] conditions. However, to our knowledge, ADCs have not yet been analysed using an FT-ICR, let alone under native-MS and solution conditions.

The purpose of this short communication is not to be an exhaustive ADC native-MS comparison between multiple instrument platforms (FT-ICR versus oa-ToF versus Orbitrap). But instead a demonstration of the capabilities of the 15 Tesla solariX FT-ICR to analyse a human IgG1 mAb conjugated with biotin, via native lysine and cysteine residues, as representative ADCs, analysed under native-MS and solution conditions. Native-MS derived DAR values are calculated and compared to those determined by the industry standard analytical method, denaturing LC-MS [30]. Finally we demonstrate reliable deconvolution of both denatured and native-MS spectra using a parsimonious model-based deconvolution algorithm [31].

Materials and Methods

Biotinylation of mAbs on lysine and cysteine residues

Briefly, for lysine conjugation (Scheme 1a) a human IgG1mAb standard was alkylated with 5 or 10-equivalents of EZ-Link sulfo-NHS-LC-biotin (Peirce). For cysteine conjugation (Scheme 1b) the mAb was partially reduced with 5 or 10-equivalents of *tris*(2-carboxyethyl)phosphine (TCEP) for 90 min at RT and then alkylated with 10-equivalents of EZ-Link iodoacetyl-LC-biotin (Pierce). This bespoke mAb conjugate was chosen over a commercial ADC, since the lysine and cysteine conjugation described herein, was easily performed on the same IgG construct to varying levels not observed in a commercial molecule. A more detailed explanation of the alkylation reaction can be found in the Supporting Information.

Native Mass Spectrometry

All native-MS experiments were performed using the 15 T solariX FT-ICR-MS instrument (Bruker Daltonics) in positive ionization mode. Mild collisional activation was performed in the source (skimmer 1, 50 V) and the hexapole collision cell (pressurized with SF_6) set to a voltage of 20 to 30 V. The MS was externally calibrated with cesium iodide over the *m/z* range 100 to

20,000. 100 scans were averaged for each spectrum and recorded at 512k (transient length 0.17 s). Prior to native-MS analysis, ADC samples were buffer exchanged into 200 mM ammonium acetate using a P6 spin column (BioRad, 732-6221). Typical native-MS working solutions were 10 µM and were introduced in to the MS using nESI gold coated glass needles (long thin wall, M956232AD1-S; Waters Corporation). All LC-MS data was acquired on an Agilent 6230 oa-TOF LC/MS system with a 1290 Infinity LC system. A more detailed explanation of all MS instrumentation and acquisition parameter can be found in the Supporting Information. The FT-ICR measured instrument resolution (FWHM) was 13,900 at *m/z* 5589 (based on the CsI cluster $Cs_{22}I_{21}$). The 6230 oa-ToF measured instrument resolution (FWHM) was 14,900 at *m/z* 2721 (based on the Agilent Tune Mix G1969-85000. ToF resolution is consistent across the *m/z* range, over which the denatured biotinylated IgG conjugate mAb is detected).

Results and Discussion

Figures 1a, b, c & d display the mAb-biotin conjugate (via native lysine and cysteine residues) as shown in Scheme 1a & b in deglycosylated form (PNGaseF treated) analysed under native-MS and solution (200 mM ammonium acetate) conditions and presented in magnitude mode (magnitude component of the output of the Fourier transformation versus *m/z* [32,33]), using a symmetric Hann apodisation function (F=0.5). In all cases a narrow charge state distribution is observed (*z* = 30+ to 24+) representative of molecular weights (MWs) ranging from 145.1 kDa to 148.2 kDa (Table 1). The observed MWs correspond to the expected mass additions of 339.5 Da (lysine conjugation) and 383.5 Da (cysteine conjugation). Importantly, well separated ADC species for each charge state are also observed and achieved using very mild activation voltages (source skimmer 50 V; collision cell 20 V). The glycosylated 5 and 10-molar biotin equivalents of the lysine conjugated molecules are displayed in the Supporting Information (Figure S1) where peak separation is achieved between the covalent biotin adduct (lysine) and the different glycoforms (G0F, G1F, G2F). In all aforementioned cases the observed charge state distributions are consistent with those previously observed for native-MS analyses of mAbs [19,27] and ADCs [11,25] and importantly are consistent with the expected charge state distribution described by de la Mora [34] based on the power relationship $z = 0.0778\ Mw^{0.5}$.

Figure 1a, Inset I, displays baseline separated charges states (z = 30+ to 26+) and differing DAR values (0 to 5) for the deglyycosylated lysine modified mAb with 5-equivalents of biotin. The overall DAR value, accounting for all observable charge states is 1.56 ±0.02 (Table 1) and was calculated from a zero-charge deconvoluted spectrum (Figure 1a, Inset II). Also detected (Figure 1a, Inset I) is low level (5%) glycation [35]. The presence of this species in this specific case is not biologically significant, however its presence highlights the ability of the 15 T solariX ICR to separate (at baseline) and identify low level species, under native solution conditions, differing in MW by only 162 Da (6 Th at *m/z* 5200). Figure 1a Insets II & III, display the deconvoluted zero-charge native (Inset II) and denatured LC-MS spectral data (Inset III; Figure S2, Supporting Information) for the biotinylated (5-molar equivalent) sample. The calculated DAR values are 1.56 ±0.02 and 2.24 ±0.02 (Table 1) respectively. As expected, the low level glycated species (+162 Da) are also well resolved in both of the zero-charged deconvoluted spectra (Figure 1a, Insets II & III). Figure 1b, represents the 10-molar biotin equivalent sample. Well resolved biotin covalent additions (DAR = 1 to 9) are easily identified on each charge state (z = 28+; Inset I) under native-MS and solution conditions, with an overall DAR value calculated to be 3.99 ±0.09 (Table 1) based on the zero-charged deconvoluted spectrum (Figure 1b, Inset II). The low level glycation, which is evident in the 5-molar equivalent sample (Figure 1a) is less evident, but still detected in both the native and denatured LC-MS data (Figure 1b, Insets I, II & III, Figure S3, Supporting Information). In the higher drug-load sample (10-molar equivalent; Figure 1b, Inset I), there are also apparent higher levels of adducting. The partially resolved trailing shoulder(s) corresponds to a range of MW increases 26 to 40 Da, based on the deconvoluted MW difference. Increased levels of adducting for higher drug load species has been previously observed by Valliere-Douglass [11].

Figures 1c and d display a deglycosylated cysteine modified mAb with 10-molar equivalents of iodoacetyl-LC-biotin under different reducing conditions (5 and 10-molar equivalents of TCEP). In both cases accurate DAR values can be identified (1 to 8 and 1 to 7 respectively; Figure 1c, Inset I & 1d, Inset I, Table S1, Supporting Information). The 10-molar TCEP equivalent clearly displays a higher level of covalent conjugation (average DAR 5.00 ±0.11, Table 1) compared to that of the 5-molar equivalent (average DAR 3.78 ±0.05, Table 1) due to a higher number of reduced cysteine residues available for alkylation. Liu [36] has previously demonstrated that interchain disulphides are more susceptible to reduction than intrachain disulphide bonds. From

an instrument perspective, these cysteine-conjugates clearly demonstrate the ability of the 15 T solariX instrument to preserve the noncovalent interactions which retain the light and heavy chain interactions, and thus transmit these ADCs, as an intact complex, through the instrument ion optics, for subsequent detection in the ICR cell. In comparison these cysteine conjugated ADCs were also analysed under denaturing LC-MS conditions (Figures S4 & S5, Table S2, Supporting Information) where only a mixture of biotin-modified light chain, modified heavy chain and intermediate versions thereof are detected; notably the fully intact ADC was not detected under denaturing LC-MS conditions, emphasizing the importance of native-MS for DAR determination of cysteine conjugated molecules [11]. When analysed under native-MS and buffer conditions (Figure 1c & d; Table S1) these synthetically generated cysteine conjugated ADCs display low levels of light chain ejection and MWs ranging from 122.1 kDa to 123.7 kDa (1LC-2HC and 1-5 Drug; Table S1, Supporting Information) detected over the *m/z* range 7,000-10,500 (Figures 1c, Inset IV & 1d, Inset IV; Table S1, Supporting Information). The intensity of these 122.1-123.7 kDa species are greater in the 5 molar-equivalent sample, suggesting the 10-molar TCEP equivalent may be less susceptible to light chain ejection. Light chain was not detected under these native-MS and solution conditions. Both the 5 and 10-molar TCEP equivalent samples display low levels of a 73 kDa species (1LC-1HC; *m/z* 3500-4500; Figure 1c, Inset II; Figure 1d, Inset II; Table S2, Supporting Information). Low levels of light chain ejection has been previously observed by Debaene [25]. However, light chain ejection was not observed by Valliere-Douglass [11]. In both of the aforementioned cases, MS data was not displayed above *m/z* 8,000, so it is unclear if the 123 kDa species (*vide supra*) was observed.

Table 1 displays the calculated DAR values for all the lysine and cysteine conjugates analysed under native-MS and solution conditions on the ICR instrument and denaturing LC-MS conditions (Figures 1a & b, Insets II & III) and MW values for the native-MS only. The average DAR values for both the native-MS ICR and denatured LC-MS of mAb-biotin conjugates were derived from the deconvoluted zero-charge spectra. It has previously been demonstrated that ion intensities observed in the unprocessed *m/z* spectra are faithfully retained in the processed deconvoluted spectra [37,38]. Therefore calculating the DAR values from a deconvoluted spectrum is fully warranted. Table S3 (Supporting information) also demonstrates the consistency of the individual charge state DAR values and the DAR values determined from spectral deconvolution; 1.58 verses 1.56, and 3.84 verses 3.99 for the 5 and 10-molar equivalent

respectively. Peak widths for both the unprocessed data and deconvoluted data for both native and denatured 5 and 10-molar equivalent are highly consistent (Figures 1a & b). A reasonable level of average DAR value consistency is observed over both MS-platforms (FT-ICR verses oa-ToF) and sample introduction methods (native-MS verses denaturing LC-MS) for the 10-molar equivalent samples: 3.99 ($\pm$0.09) versus 4.43 ($\pm$0.01) respectively, and lower for the 5-molar equivalent sample 1.56 ($\pm$0.02) versus 2.24 ($\pm$0.02) respectively. All native-MS conditions display a lower number of dominant charge states (z = 24+ to 30+; Figures 1a & 1b). Only 1 to 5 biotin modifications on lysine were observed from native-MS of the 5-molar equivalent sample. This is a lower DAR value than that obtained from the denatured LC-MS 5-molar equivalent data, where up to 6 covalent biotin modifications (Figure 1a, Insets II & III) can be easily identified. The number of covalent modifications is highly comparable for the 10-molar equivalent mAb conjugate molecule analysed in both native and denaturing LC-MS conditions. It would therefore appear that higher DAR value species (DAR = 5 and 6; Figure 1a, Inset III) for the 5-molar equivalent sample, are only observed under denaturing LC-MS conditions (0.1% formic acid and acetonitrile) suggesting their ionization efficiencies under reversed phase and denaturing LC-MS conditions are higher than those under native-MS and solution conditions. Under the aforementioned denaturing LC-MS conditions, protein gas-phase [39-41] and solution [42] conformations are more extended and unfolded, the effect of which is most dramatic for the lowest DAR value species (*vide infra*). This increased level of unfolding results in improved detection efficiencies most likely due to the improved signal-to-noise ratio that is typically observed higher for denaturing spectra. One must also consider the increased levels of ADC adducting when the ADC is in a folded state. Under native-MS and solution conditions, protein adducting from sodium for example, can reduce overall molecular ion abundances [43,44], the results of which are particularly acute for the low level species (DARs 5 & 6). Chen [45] has also postulated increased hydrophobicity levels for higher drug load molecules, resulting in reduced ionization efficiencies. Also observed by multiple groups are significant differences in calculated DAR values obtained using different analytical techniques, such as hydrophobic interaction chromatography versus native-MS [45] and native-IM-MS [25].

The DAR values calculated for the denatured mAb will also be inherently more accurate and consistent, since a higher number of charge states are being selected for deconvolution (Figure S2 & S3, Supporting Information). Additionally, the ESI process is significantly aided by the

pneumatic nebulization and desolvation which is heated and operated at a significantly higher flow rate, reducing ion current fluctuations. These variations are potentially exacerbated when analysing under nESI conditions. As a result, more accurate DAR values can be obtained with lower SD values (Table 1) when using standard ESI conditions as opposed to nESI native-MS conditions.

Conclusion

The data presented herein demonstrates the ability of the solariX 15 Tesla FT-ICR to transmit and detect mAb-biotin-conjugates from both lysine and cysteine modification, under native-MS and solution conditions. Importantly, baseline separation of every charge state and each incremental covalent biotin conjugation, including separation between glycoforms and covalent biotin adducts was achieved. Average DAR values for the lysine conjugates show variation across ICR and oa-ToF instrument platforms (particularly for the lower biotin-load; 5-molar equivalents; 3.99 ±0.09 versus 4.43 ±0.01) where one data set was analysed under native-MS and solution conditions and the other by denaturing LC-MS; calculated DAR values (n=3) are consistently lower under native-MS and buffer conditions, with a higher SD values. These observation, and those by others (*vide supra*) are consistent, in that the calculated DAR value can vary, depending on which analysitcal technique is used to make the measurement. Chen [45] described a DAR value variation of 0.5 between native-MS and a HIC method for a reduced cysteine interchain ADC molecules. Accurate DAR values for the cysteine conjugate were also achieved (3.78 ±0.05 and 5.00 ±0.11), where the heavy and light chains are held together by a mixture of noncovalent interactions and disulphide bonds. This further highlights the apparent "gentleness" of the ICRs ion optics and pressure gradients for transmitting native-like protein ions from the nanoESI source region through to the instrument to the ICR cell. The native cysteine biotin conjugate (145.5 to 148.0 kDa) cannot remain as a fully intact molecule under denaturing LC-MS conditions, further highlighting the advantages of native-MS analysis on the ICR platform. We have also demonstrated the use of a single algorithm which is able to deconvolute both denatured and native-MS spectra, without the need for parameter adjustment. This is important, since charge states are generally more adducted under native-MS conditions

and previous Maximum Entropy based algorithms [37] have struggled to deconvolute native MS-spectra with these increased levels of added complexity [46]

A limited number of high mass applications have been demonstrated by FT-ICR analysis[47,48]. However, over the past 5 years more native gas-phase protein and high mass applications have been described by FT-ICR where the applications have ranged from mAbs [27], to membrane proteins [49,50], nanodiscs [49,51,52] and native protein top-down analyses [53,54]. The native-MS data presented herein further demonstrates the enabling capabilities of an unmodified FT-ICR platform for native high mass (and high *m/z*) analysis, producing mAb conjugate data equivalent in quality to that previously only thought to be achievable using oa-ToF analysers [55-59] and more recently the Orbitrap [19,23,26,60]. The user has the ability to acquire data at ultrahigh resolution. One can also perform ECD [53] and IRMPD [49,61] activation experiments on protein analysed under native-MS and solution conditions, if desired. The described 15 T solariX FT-ICR MS instrument is clearly a *bona fide* instrument for enabling high mass, native gas-phase protein analyses.

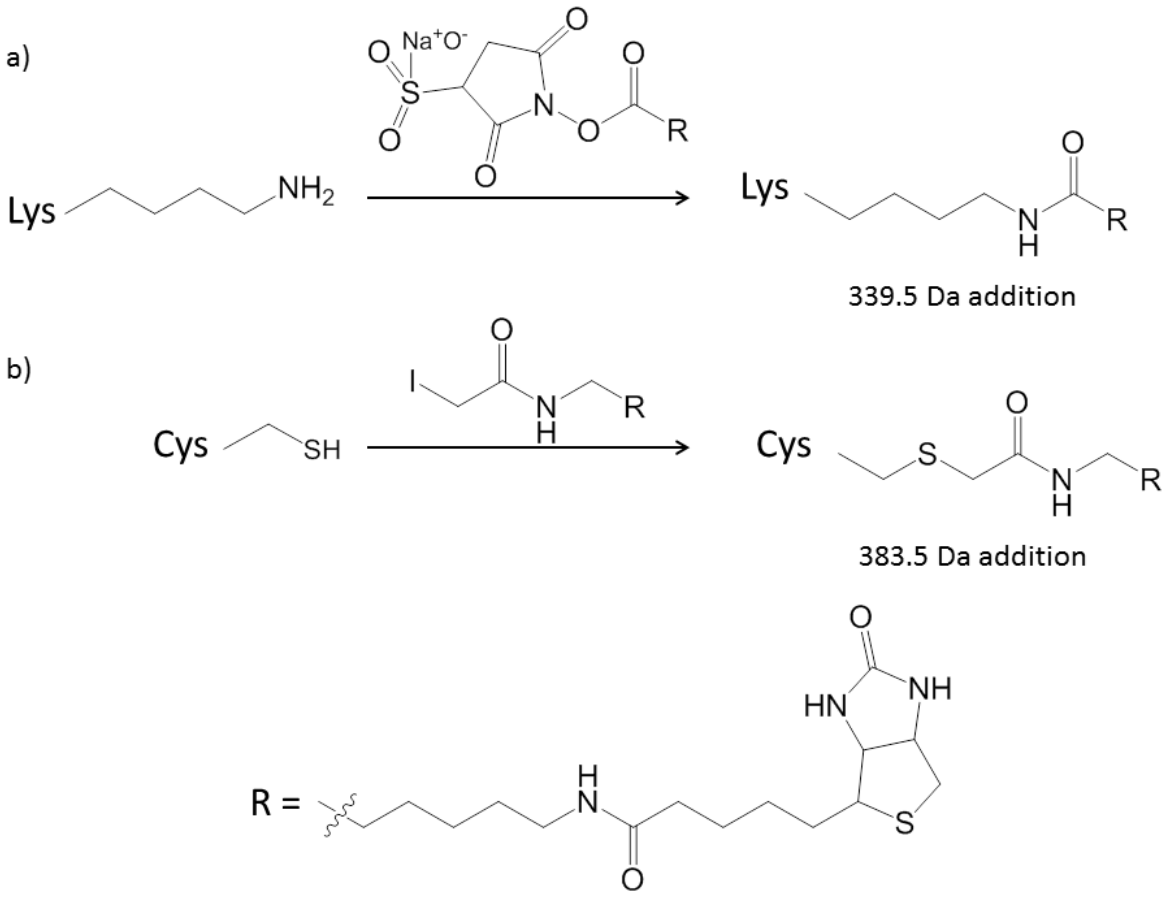

Scheme 1. The synthetic scheme of lysine and cysteine conjugation used to covalently modify the IgG 1 mAb described herein. Sulfo-NHS-LC-biotin and lysine conjugation are shown in (a). Iodoacetyl-LC-biotin and cysteine conjugation are shown in (b). Observed MW additions to the IgG1 mAb, for a single conjugation are annotated (in Da, average MW).

Native FT-ICR MS Spectra of the mAb Conjugate Molecule, Analysed over the *m/z* Range 3,500 to 10,500

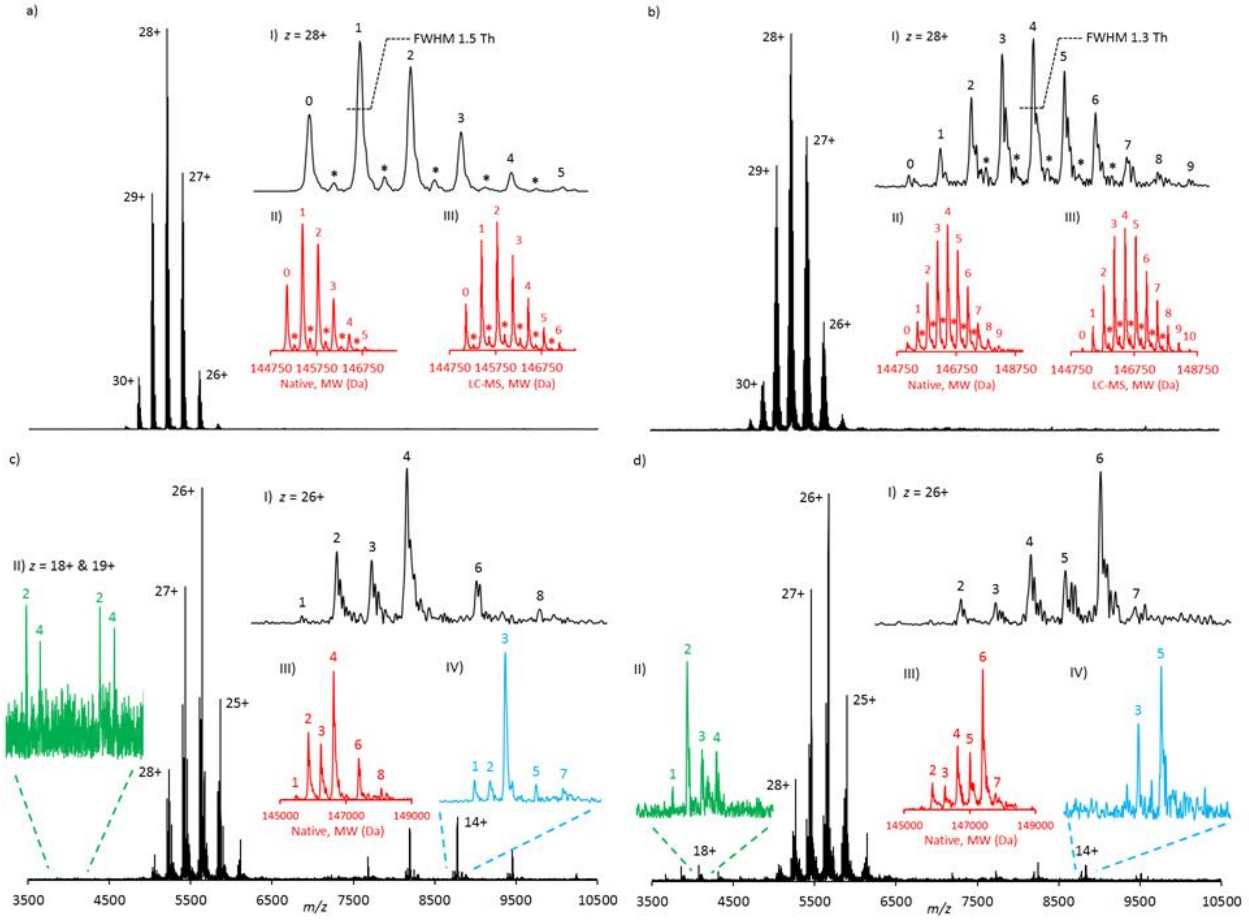

Figure 1. a) 5-molar equivalent lysine-biotin conjugate; b) 10-molar equivalent lysine-biotin conjugate; c) 5-molar equivalent TCEP, 10-molar equivalent cysteine-biotin conjugate; d) 10-molar equivalent TCEP, 10-molar equivalent cysteine-biotin conjugate; DAR values are annotated on selected charge states and all deconvoluted spectra. *Represents a +162 Da glycation mass increase. Data is displayed as magnitude mode using a symmetric Hann apodisation function. Deconvolution was performed using the PMI deconvolution algorithm. The annotated DAR values in Insets c and d, III and IV are consistent with the number of covalently attached biotin moieties to the specific species and not the full intact initial mAb

conjugate molecule. Peak widths at half height of for *z*=28+ are annotated. Peak widths at half height for the equivalent deconvoluted data range from 39.2 – 41.1 Th.

	Native-MS DAR (ave)	SD	LC-MS DAR (ave)	SD	Native MW (Da)
mAb lysine conjugate molecule (5-eq biotin)	1.56	0.02	2.24	0.02	145,100.00 ± 0.01 (DAR=0) 145,439.33 ± 1.15 (DAR=1) 145,780.00 ± 2.00 (DAR=2) 146,118.67 ± 1.14 (DAR=3) 146,456.00 ± 2.00 (DAR=4)* 146,796.00 ± 2.00 (DAR=5)*
mAb lysine conjugate molecule (10-eq biotin)	3.99	0.09	4.43	0.01	145,109.04 ± 7.91 (DAR=0)* 145,443.99 ± 5.28 (DAR=1)* 145,780.66 ± 1.16 (DAR=2) 146,120.00 ± 2.00 (DAR=3) 146,460.00 ± 0.01 (DAR=4) 146,798.66 ± 1.15 (DAR=5) 147,139.33 ± 1.15 (DAR=6) 147,477.33 ± 1.15 (DAR=7) 147,818.67 ± 5.04 (DAR=8)* 148,161.34 ± 4.14 (DAR=9)*
mAb cysteine conjugate molecule (5-eq biotin; 5-eq TCEP)	3.78	0.05	-	-	145,478.00 ± 2.82 (DAR=1)* 145,861.99 ± 0.00 (DAR=2) 146,243.99 ± 0.00 (DAR=3) 146,630.00 ± 0.00 (DAR=4) 147,394.00 ± 0.00 (DAR=6) 148,079.01 ± 4.24 (DAR=8)*
mAb cysteine conjugate molecule (5-eq biotin; 10-eq TCEP)	5.00	0.11	-	-	145,861.01 ± 0.01 (DAR=2)* 146,245.99 ± 2.83 (DAR=3)* 146,626.99 ± 1.39 (DAR=4) 147,010.00 ± 0.01 (DAR=5) 147,395.00 ± 1.41 (DAR=6) 147,779.99 ± 8.47 (DAR=7)*

Table 1. Drug-to-antibody ratios (DARs) and deconvoluted MWs reported for the intact IgG1 mAb lysine and cysteine conjugate molecule analysed under native-MS (FT-ICR; magnitude mode, asymmetric apodisation) and denaturing LC-MS conditions. DAR values calculated from deconvoluted MW peak intensities. DAR and MW standard deviation values are derived from *n* = 3. DAR values were not acquired under LC-MS conditions for the cysteine conjugate since an

intact MW cannot be obtained under denaturing LC-MS conditions. *Indicates low native-MS signal in both unprocessed and deconvoluted data.

Acknowledgements

The authors would like to thank Marshall Bern, Eric Carlson and Yong Joo Kil from Protein Metrics Inc. for all of their useful collaborative discussions and help during native spectral deconvolution. Support from the US National Institutes of Health (R01GM103479 and S10RR028893) and the US Department of Energy (UCLA/DOE Institute for Genomics and Proteomics; DE-FC03-02ER63421) to JAL is acknowledged.

Supporting Information

Conditions for lysine and cysteine biotinylation, MS instrument conditions, Native nESI FT-ICR MS data for the glycosylated mAb conjugates, unprocessed and deconvoluted LC-MS oa-ToF data for the glycosylated and deglycosylated mAb conjugates, deconvoluted MWs native-MS and LC-MS oa-ToF analysis of the cysteine-biotin conjugates, unprocessed and deconvoluted LC-MS oa-ToF data for the cysteine-biotin conjugates, schematic representations of the lysine and cysteine conjugates and DAR values derived for each charge state.

References

(1) Beck, A.; Goetsch, L.; Dumontet, C.; Corvaia, N. *Nature reviews. Drug discovery* **2017**, *16*, 315-337.
(2) Ornes, S. *Proc Natl Acad Sci U S A* **2013**, *110*, 13695.
(3) Mullard, A. *Nature reviews. Drug discovery* **2013**, *12*, 329-332.
(4) Diamantis, N.; Banerji, U. *British journal of cancer* **2016**, *114*, 362-367.
(5) Hamblett, K. J.; Senter, P. D.; Chace, D. F.; Sun, M. M.; Lenox, J.; Cerveny, C. G.; Kissler, K. M.; Bernhardt, S. X.; Kopcha, A. K.; Zabinski, R. F.; Meyer, D. L.; Francisco, J. A. *Clin Cancer Res* **2004**, *10*, 7063-7070.
(6) Sun, M. M.; Beam, K. S.; Cerveny, C. G.; Hamblett, K. J.; Blackmore, R. S.; Torgov, M. Y.; Handley, F. G.; Ihle, N. C.; Senter, P. D.; Alley, S. C. *Bioconjug Chem* **2005**, *16*, 1282-1290.
(7) Chih, H. W.; Gikanga, B.; Yang, Y.; Zhang, B. *Journal of pharmaceutical sciences* **2011**, *100*, 2518-2525.
(8) Baldwin, A. D.; Kiick, K. L. *Bioconjug Chem* **2011**, *22*, 1946-1953.
(9) Kim, M. T.; Chen, Y.; Marhoul, J.; Jacobson, F. *Bioconjug Chem* **2014**, *25*, 1223-1232.
(10) Panowski, S.; Bhakta, S.; Raab, H.; Polakis, P.; Junutula, J. R. *MAbs* **2014**, *6*, 34-45.
(11) Valliere-Douglass, J. F.; McFee, W. A.; Salas-Solano, O. *Anal Chem* **2012**, *84*, 2843-2849.
(12) Guo, J.; Kumar, S.; Chipley, M.; Marcq, O.; Gupta, D.; Jin, Z.; Tomar, D. S.; Swabowski, C.; Smith, J.; Starkey, J. A.; Singh, S. K. *Bioconjug Chem* **2016**, *27*, 604-615.
(13) Sharon, M.; Robinson, C. V. *Annu Rev Biochem* **2007**, *76*, 167-193.
(14) Heck, A. J. *Nature methods* **2008**, *5*, 927-933.
(15) Benesch, J. L.; Ruotolo, B. T. *Curr Opin Struct Biol* **2011**, *21*, 641-649.
(16) Ruotolo, B. T.; Benesch, J. L.; Sandercock, A. M.; Hyung, S. J.; Robinson, C. V. *Nat Protoc* **2008**, *3*, 1139-1152.
(17) Pacholarz, K. J.; Porrini, M.; Garlish, R. A.; Burnley, R. J.; Taylor, R. J.; Henry, A. J.; Barran, P. E. *Angew Chem Int Ed Engl* **2014**, *53*, 7765-7769.
(18) Campuzano, I. D. G.; Larriba, C.; Bagal, D.; Schnier, P. D. *ACS Symposium Series* **2015**, *1202*, 75-112.
(19) Rose, R. J.; Damoc, E.; Denisov, E.; Makarov, A.; Heck, A. J. *Nature methods* **2012**, *9*, 1084-1086.
(20) Shaw, J. B.; Brodbelt, J. S. *Anal Chem* **2013**, *85*, 8313-8318.
(21) Hengel, S. M.; Sanderson, R.; Valliere-Douglass, J.; Nicholas, N.; Leiske, C.; Alley, S. C. *Anal Chem* **2014**, *86*, 3420-3425.
(22) Valliere-Douglass, J. F.; Hengel, S. M.; Pan, L. Y. *Molecular pharmaceutics* **2015**, *12*, 1774-1783.
(23) Belov, M. E.; Damoc, E.; Denisov, E.; Compton, P. D.; Horning, S.; Makarov, A. A.; Kelleher, N. L. *Anal Chem* **2013**, *85*, 11163-11173.
(24) Dyachenko, A.; Wang, G.; Belov, M.; Makarov, A.; de Jong, R. N.; van den Bremer, E. T.; Parren, P. W.; Heck, A. J. *Anal Chem* **2015**, *87*, 6095-6102.

(25) Debaene, F.; Boeuf, A.; Wagner-Rousset, E.; Colas, O.; Ayoub, D.; Corvaia, N.; Van Dorsselaer, A.; Beck, A.; Cianferani, S. *Anal Chem* **2014**, *86*, 10674-10683.
(26) van de Waterbeemd, M.; Snijder, J.; Tsvetkova, I. B.; Dragnea, B. G.; Cornelissen, J. J.; Heck, A. J. *J Am Soc Mass Spectrom* **2016**, *27*, 1000-1009.
(27) Jones, L. M.; Zhang, H.; Cui, W.; Kumar, S.; Sperry, J. B.; Carroll, J. A.; Gross, M. L. *J Am Soc Mass Spectrom* **2013**, *24*, 835-845.
(28) Marzilli, L.; Ly, M.; Stephens, E.; DeGruttola, H. S.; Saati, A. E.; Rouse, J. C. *PITTCON Conference and Expo, (260-3), Atlanta, Georgia* **2016**.
(29) Shaw, J. B.; Lin, T. Y.; Leach, F. E., 3rd; Tolmachev, A. V.; Tolic, N.; Robinson, E. W.; Koppenaal, D. W.; Pasa-Tolic, L. *J Am Soc Mass Spectrom* **2016**, *27*, 1929-1936.
(30) Wakankar, A.; Chen, Y.; Gokarn, Y.; Jacobson, F. S. *MAbs* **2011**, *3*, 161-172.
(31) Bern, M. W.; Kil, Y. J.; Carlson, E.; Kletter, D.; Tang, W.; Becker, C. *American Society for Mass Spectrometery Annual Conference, 2016, San Antonio, Texas* **2016**.
(32) Marshall, A. G.; Hendrickson, C. L.; Jackson, G. S. *Mass Spectrom Rev* **1998**, *17*, 1-35.
(33) Kilgour, D. P.; Van Orden, S. L. *Rapid Commun Mass Spectrom* **2015**, *29*, 1009-1018.
(34) J., d. l. M. F. *Analytica Chimica Acta* **2000**, *406*, 93-104.
(35) Haberger, M.; Bomans, K.; Diepold, K.; Hook, M.; Gassner, J.; Schlothauer, T.; Zwick, A.; Spick, C.; Kepert, J. F.; Hienz, B.; Wiedmann, M.; Beck, H.; Metzger, P.; Molhoj, M.; Knoblich, C.; Grauschopf, U.; Reusch, D.; Bulau, P. *MAbs* **2014**, *6*, 327-339.
(36) Liu, H.; Chumsae, C.; Gaza-Bulseco, G.; Hurkmans, K.; Radziejewski, C. H. *Anal Chem* **2010**, *82*, 5219-5226.
(37) Ferrige, A. G.; Seddon, M. J.; Green, B. N.; Jarvis, S. A.; Skilling, J. *Rapid Commun Mass Spectrom* **1992**, *6*, 707-711.
(38) Debaene, F.; Wagner-Rousset, E.; Colas, O.; Ayoub, D.; Corvaia, N.; Van Dorsselaer, A.; Beck, A.; Cianferani, S. *Anal Chem* **2013**, *85*, 9785-9792.
(39) Katta, V.; Chait, B. T. *Rapid Commun Mass Spectrom* **1991**, *5*, 214-217.
(40) Clemmer, D. E.; Hudgins, R. R.; Jarrold, M. F. *Journal of the American Chemical Society* **1995**, *117*, 10141-10142.
(41) Konermann, L.; Douglas, D. J. *Rapid Commun Mass Spectrom* **1998**, *12*, 435-442.
(42) Knubovets, T.; Osterhout, J. J.; Klibanov, A. M. *Biotechnology and bioengineering* **1999**, *63*, 242-248.
(43) Flick, T. G.; Cassou, C. A.; Chang, T. M.; Williams, E. R. *Anal Chem* **2012**, *84*, 7511-7517.
(44) Cassou, C. A.; Williams, E. R. *Analyst* **2014**, *139*, 4810-4819.
(45) Chen, J.; Yin, S.; Wu, Y.; Ouyang, J. *Anal Chem* **2013**, *85*, 1699-1704.
(46) Morgner, N.; Robinson, C. V. *Anal Chem* **2012**, *84*, 2939-2948.
(47) Amster, J. I.; McLafferty, F. W.; Castro, M. E.; Russell, D. H.; Cody, R. B.; Ghaderi, S. *Analytical Chemistry* **1986**, *58*, 483-485.
(48) Lebrilla, C. B.; Wang, D. T.; Hunter, R. L.; McIver, R. T., Jr. *Anal Chem* **1990**, *62*, 878-880.
(49) Campuzano, I. D.; Li, H.; Bagal, D.; Lippens, J. L.; Svitel, J.; Kurzeja, R. J.; Xu, H.; Schnier, P. D.; Loo, J. A. *Anal Chem* **2016**, *88*, 12427-12436.
(50) Lippens, J. L.; Nshanian, M.; Spahr, C.; Egea, P. F.; Loo, J. A.; Campuzano, I. D. G. *J Am Soc Mass Spectrom* **2017**, doi: 10.1007/s13361-017-1799-4.
(51) Marty, M. T.; Zhang, H.; Cui, W.; Blankenship, R. E.; Gross, M. L.; Sligar, S. G. *Anal Chem* **2012**, *84*, 8957-8960.

(52) Marty, M. T.; Zhang, H.; Cui, W.; Gross, M. L.; Sligar, S. G. *J Am Soc Mass Spectrom* **2014**, *25*, 269-277.
(53) Li, H.; Wolff, J. J.; Van Orden, S. L.; Loo, J. A. *Anal Chem* **2014**, *86*, 317-320.
(54) Li, H.; Wongkongkathep, P.; Van Orden, S. L.; Ogorzalek Loo, R. R.; Loo, J. A. *J Am Soc Mass Spectrom* **2014**, *25*, 2060-2068.
(55) Sobott, F.; Hernandez, H.; McCammon, M. G.; Tito, M. A.; Robinson, C. V. *Anal Chem* **2002**, *74*, 1402-1407.
(56) Sobott, F.; Robinson, C. V. *Internation journal of mass spectrometry* **2004**, *236*, 25-32.
(57) Chernushevich, I. V.; Thomson, B. A. *Anal Chem* **2004**, *76*, 1754-1760.
(58) Campuzano, I.; Giles, K. *Nanospray Ion Mobility Mass Spectrometry of Selected High Mass Species. Nanoproteomics: Methods and Protocols, Methods in Molecular Biology, (Eds: S. A. Toms, R. Weil), Humana Press, a part of Springer Science+Business Media, LLC, New York* **2011**, *790*, 57-70.
(59) Snijder, J.; Rose, R. J.; Veesler, D.; Johnson, J. E.; Heck, A. J. *Angew Chem Int Ed Engl* **2013**, *52*, 4020-4023.
(60) Gault, J.; Donlan, J. A.; Liko, I.; Hopper, J. T.; Gupta, K.; Housden, N. G.; Struwe, W. B.; Marty, M. T.; Mize, T.; Bechara, C.; Zhu, Y.; Wu, B.; Kleanthous, C.; Belov, M.; Damoc, E.; Makarov, A.; Robinson, C. V. *Nature methods* **2016**, *13*, 333-336.
(61) Mikhailov, V. A.; Liko, I.; Mize, T. H.; Bush, M. F.; Benesch, J. L.; Robinson, C. V. *Anal Chem* **2016**, *88*, 7060-7067.

For Table of Contents Only